

Input Amplifiers for Optical PCM Receivers

By J. E. GOELL

(Manuscript received March 1, 1974)

This paper describes the noise performance of input amplifiers for optical pulse-code-modulation repeaters. The noise is treated in terms of an effective noise generator in parallel with the photocurrent induced in the detector and the effective noise, in turn, is related to error performance. The analysis applies to both conventional and integrating front ends. Both field effect and bipolar transistor amplifiers are treated. For the latter, an optimum bias current that minimizes the effect of thermal noise is derived. Finally, predicted and measured performance are compared for silicon field-effect transistor input amplifiers at 6.3 Mb/s and 50 Mb/s, and for bipolar transistor and GaAs field-effect transistor input amplifiers at 274 Mb/s.

I. INTRODUCTION

The factors which limit the performance of an optical receiver are optical quantum noise, leakage noise of the detector, thermal noise introduced by the detector load resistor, and various forms of noise introduced by the input amplifier. If an avalanche detector is used, the leakage noise has two components—one which is gain independent and the other which is gain dependent. In addition, the gain process introduces a signal-dependent noise. In high-speed pulse-code-modulation (PCM) receivers, input-amplifier noise plays an important role in the determination of system performance. If leakage current is negligible, it can be shown^{1,2} that without avalanche gain the required signal power to achieve a given error probability varies as the square root of the thermal noise power and with optimum avalanche gain with the sixth root of the thermal noise power. Furthermore, the optimal avalanche gain varies as the cube root of the thermal noise power.*

* These results assume an excess noise coefficient of 0.5.

In applications employing a detector with a capacitive impedance such as nuclear particle counters³ and television camera input amplifiers,⁴ an approach has been employed in which the input circuit integrates the signal and the signal is equalized after amplification. Personick² has analyzed the performance of PCM repeaters with integrating front ends and Goell has experimentally verified some of his results at 6.3 Mb/s.⁵

The noise performance of an amplifier is often stated in terms of noise figure. This approach is attractive when thermal noise can be reduced by matching the source impedance to the optimum noise impedance of the amplifier. For optical receivers and other systems with a capacitive source the noise of the source is often a negligible portion of the total thermal noise, and the noise contributed by transformer losses would more than negate the advantage gained by transformation. For this case, noise figure, which is inversely proportional to source noise power, is a poor figure of merit and it is better to treat the noise directly.

The approach chosen here is to describe the noise of the amplifier by an equivalent input noise current generator which produces the same noise at the output as the internal sources of the amplifier. The intermediate step of finding a short-circuit input noise current generator and open-circuit input noise voltage generator is dispensed with here because it does not contribute to physical understanding when the noise figure concept is not employed.

If the linear portion of the receiver is modeled by a cascade of an amplifier, an equalizer to give a flat frequency response in the band of interest, and a filter to set the noise bandwidth and control the pulse response, then the equivalent current is a particularly convenient way to express the noise. This approach is conceptually simple, the effect of equalization is implicitly included, and filtering has the same effect on the equivalent noise as on the signal.

The error performance of a PCM receiver can be related to the ratio of the peak signal to rms noise ratio at the regenerator. It will be shown that this ratio is equal to the ratio of the average received signal power to an effective noise current which can be readily derived from the equivalent input noise current.

In the previously mentioned work by Personick the amplifier noise was modeled by the series voltage and shunt current noise generator. Results were given only for field effect transistor (FET) input amplifiers. In this paper the noise of both field effect and bipolar transistor amplifiers is analyzed. The effect of spreading resistance and load

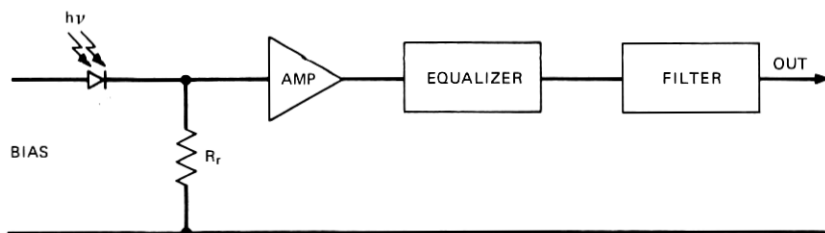


Fig. 1—Typical input circuit of an optical repeater.

noise is included and the application of the method to cases in which the noise of more than one stage is significant is described. The approach is used to compare the performance of silicon bipolar and field effect transistors and GaAs field effect transistors as a function of bit rate. Theoretical predictions are compared with measured results for silicon FET input amplifiers at 6.3 Mb/s and 50 Mb/s⁶ and for bipolar transistor and GaAs FET input amplifiers at 274 Mb/s.

II. CALCULATION OF EQUIVALENT NOISE

A model of the initial stages of a typical optical receiver is shown in Fig. 1. The resistor R_r is provided to return the detector bias current to its source. Equalization is provided to compensate for the frequency dependence of the amplifier gain, and filtering is provided to limit the noise bandwidth and shape the signal. For the cases to be described here, it is convenient to think in terms of an equalizer to give a flat frequency response followed by a filter which describes the frequency dependence of the transfer characteristic of the receiver, although in practice they can be combined. In some applications, such as where matched filtering is to be employed, another approach might be used.

The detector circuit without avalanche gain can be modeled as shown in Fig. 2. Here i_p is the induced photocurrent, C_j the detector

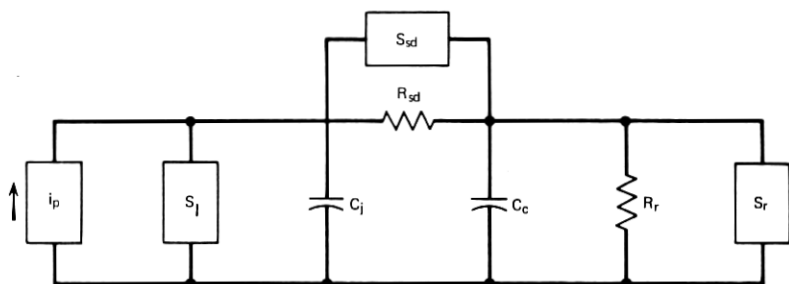


Fig. 2—Detector circuit.

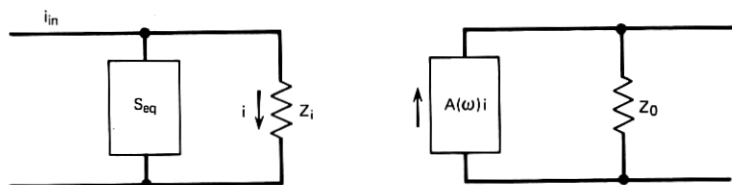


Fig. 3—Equivalent noise circuit.

junction capacitance, R_{sd} the diode spreading resistance and S_{sd} the noise current spectral density associated with it, C_c the capacitance of the interconnection circuit, S_r the noise current spectral density of the dc return resistor, and S_l the spectral density of the gain-independent diode-leakage noise current.* With avalanche gain, i_p is the photocurrent multiplied by the mean gain, \bar{g} .

The performance of any linear amplifier can be described by the equivalent circuit of Fig. 3. Here, the impedance Z_i is the parallel combination of the input impedance of the circuit and the output impedance of the preceding circuit, and $A(\omega)$ is the current amplification of the stage. S_{eq} is the frequency-dependent equivalent noise current spectral density of the noise current generator which when applied to the input gives the same output noise spectral density as the internal noise generators.

An equivalent circuit which applies to both bipolar and field-effect transistors is shown in Fig. 4. Spreading resistance has been ignored for the present, but will be analyzed later as a separate stage.

The equivalent noise current spectral density is given by

$$S_{eq} = S_{eq1} + S_{eq2}, \quad (1)$$

where S_{eq1} is the contribution to S_{eq} of S_1 , the emitter (source) noise current spectral density, and S_{eq2} is the contribution to S_{eq} of S_2 , the collector (drain) noise current spectral density. The calculation of S_{eq1} and S_{eq2} for common emitter (source), collector (drain), and base (gate) stages is described in the appendix. A comparison of amplifier configuration is also given.

At low frequencies, that is, when the transit time of carriers through the device is short compared to the period of the signal, for a field-effect transistor at pinch-off

$$S_1 = 4kT\theta(\omega c_0)^2/g_m + 2eI_0 \quad (2)$$

* The effect of the gain-dependent leakage noise has been described by Personick.²

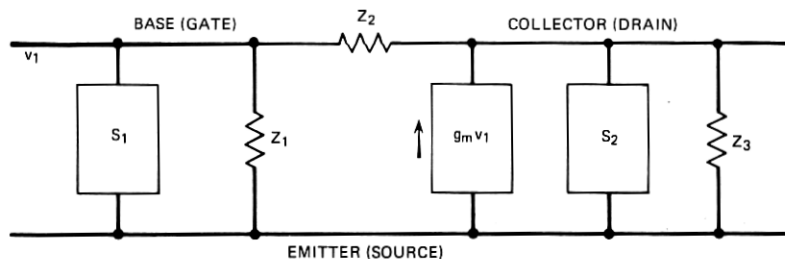


Fig. 4—Equivalent circuit for both bipolar and field effect transistors.

and

$$S_2 = 4kT\Gamma g_m, \quad (3)$$

where T is the temperature, g_m is the transconductance, I_g is the gate leakage current, c_g is the gate capacitance, and k is Boltzmann's constant.⁷ For junction field-effect transistors, $\Gamma = \frac{2}{3}$ and θ varies from $\frac{1}{10}$ to $\frac{4}{15}$.⁸ With currently available devices, drain noise has been found to predominate with an untuned input circuit.

At very low frequencies account must also be taken at $1/f$ noise. The $1/f$ noise region for junction field-effect transistors extends to a few hundred kilohertz, while for metal-oxide semiconductor field effect transistors it can extend to above 10 MHz. For GaAsFETs intervalley scattering adds an additional component of noise. For this case $\Gamma = 1.1$.⁹

For bipolar transistors with short base transit time, the input and output noise generator spectral densities are given by

$$S_1 = 2eI_b, \quad (4)$$

$$S_2 = 2eI_c, \quad (5)$$

where I_b is the base current and I_c is the collector current.⁷ The above applies for the case of short base transit time and the base current much greater than the reverse base saturation current.

III. EFFECTIVE NOISE IN PCM RECEIVERS

For PCM systems, performance is measured in terms of required power to achieve a specified error probability and the error probability is determined from the ratio of the peak signal to the rms noise at the regenerator input. In this section the relationship between the peak-signal-to-rms-noise ratio, the average received signal, and the equivalent noise will be described.

We shall assume that the detected photocurrent, an undistorted version of the transmitted signal, is given by

$$\sum_{k=-\infty}^{\infty} T_b b_k I_{av} h_p(t - kT_b),$$

where

$$\int_{-\infty}^{\infty} h_p(t - kT_b) dt = 1,$$

$b_k = 0, 1$ depending on the signal statistics, T_b is the bit interval, and $I_{av}T_b$ is the detected charge if a single pulse were received. It is assumed that the transmitted pulses are distinct.

The output signal is given by

$$\sum_{k=-\infty}^{\infty} b_k h_m h_o(t - kT_b),$$

where $h_o(t)$ has been normalized to have unit peak amplitude and h_m is the peak output signal current. It will be assumed that intersymbol interference is negligible, that is, that at the sampling instant, t_s ,

$$\begin{aligned} h_o(t_s - kT_b) &= 0 \\ k &= \pm 1, \pm 2, \dots \end{aligned}$$

An inconsequential time displacement has been ignored. Then the transfer function is given by

$$A(\omega) = \frac{h_m H_o(\omega)}{T_b I_{av} H_p(\omega)}, \quad (6)$$

where $H_p(\omega)$ and $H_o(\omega)$ are the Fourier transforms of $h_p(t)$ and $h_o(t)$, respectively. The mean-square noise after amplification and filtering is given by

$$\overline{n^2} = \frac{1}{2\pi} \int_0^{\infty} |A(\omega)|^2 S_{eq}(\omega) d\omega.$$

Substituting the mean-square noise into eq. (6) gives the peak-signal-to-rms-noise ratio

$$\frac{h_m}{\sqrt{\overline{n^2}}} = \frac{I_{av}}{\sqrt{i_{eff}^2}}, \quad (7)$$

where

$$i_{eff}^2 = \frac{1}{2\pi T_b^2} \int_0^{\infty} \left| \frac{H_o(\omega)}{H_p(\omega)} \right|^2 S_{eq} d\omega. \quad (8)$$

Thus the quantity $\sqrt{i_{\text{eff}}^2}$ is an effective noise current which relates the thermal noise to the average induced photocurrent.

For the case where most of the noise originates in the first amplifier stage we will see that under conditions which apply in several cases of interest the equivalent noise can be expanded in the Taylor series

$$S_{\text{eq}}(\omega) = \sum_j \alpha_j(\omega) g_j.$$

It is then convenient to put the effective noise in the form

$$\overline{i_{\text{eff}}^2} = f_b \sum_j \alpha_j (2\pi f_b)^j g_j, \quad (9)$$

where

$$g_j = \frac{f_b^{1-j}}{(2\pi)^{j+1}} \int_0^\infty \left| \frac{H_o(\omega)}{H_p(\omega)} \right|^2 \omega^j d\omega \quad (10)$$

and $f_b = 1/T_b$. The normalization ratio was chosen so that the g 's depend only on the shape of the pulse relative to the bit interval, not on the bit interval.

It can be shown^{2,5} that for binary PCM with an avalanche detector the power required to achieve a specified error probability, P_e , is given by

$$p = \frac{h\nu Q}{2\eta} \left[\frac{Q\bar{g}^2 f_b}{\bar{g}^2} + \frac{2}{\bar{g}e} \sqrt{i_{\text{eff}}^2} \right], \quad (11)$$

where

η = detector quantum efficiency,

e = electronic charge,

ν = optical frequency,

β = detector quantum efficiency,

\bar{g} = mean detector gain,

\bar{g}^2 = mean-squared detector gain,

and

$$G = \sqrt{2} \operatorname{erfc}^{-1}(2P_e).$$

The function erfc is the error function complement. For a gainless detector when thermal noise predominates, the first term in the bracket of eq. (11) can be neglected.

A value of \bar{g} exists¹ which minimizes p . The ratio of \bar{g}^2/\bar{g}^2 can be approximated* by \bar{g}^x . Then the value of \bar{g} which minimizes p is given by

$$g_{\text{opt}} = \left(\frac{2\sqrt{i_{\text{eff}}^2}}{xeQf_b} \right)^{1/(x+1)} \quad (12)$$

and the required power at optimum gain is given by

$$P_{\text{opt}} = \frac{h\nu Q^{(x+2)/(x+1)}}{\eta e} \left(\frac{xe f_b}{2} \right)^{1/(x+1)} \left(1 + \frac{1}{x} \right) \bar{i}_{\text{eff}}^{-x/(2x+2)} \quad (13)$$

IV. APPLICATIONS

In this section, the effective noise for both field effect and bipolar transistors will be described. Emphasis will be placed on conditions encountered in receivers operating in the 1-Mb/s to 1-Gb/s range. It will be assumed that most of the noise originates in or before the first amplifier stage. Corrections for the load, subsequent stage, and spreading resistance noises will be included.

Both detectors and transistors have distributed junction capacitance and series resistance followed by a case capacitance. However, at the frequencies to be covered here the equivalent circuit can be approximated by capacitors across the detector source and transistor base (gate) separated by the total spreading resistance of both devices. The spreading resistance can be considered as a separate stage with a transfer function $A(\omega)$ given by

$$A(\omega) = \frac{1}{1 + j\omega C_d R_s}$$

and noise current spectral density

$$S_s = 4kT\omega^2 C_d^2 R_s,$$

where C_d is capacitance across the detector source.

The gain-independent leakage current I_d can be accounted for by a noise spectral density

$$S_{\text{eqd}} = 2eI_d$$

in parallel with the detector current generator. Noise of spectral density S_r is contributed by the return resistor, R_r , which will be assumed to be on the amplifier side of R_s . This assumption is valid as long as the contribution of R_s to the noise is small.

* Silicon detectors with x between 0.3 and 0.5 are available today commercially.

The total equivalent noise current spectral density can be written as

$$S_{\text{eq}} = S_s + S_{\text{eq}d} + \frac{S_{\text{eq}1} + S_r + S_{\text{eq}2}}{|A(\omega)|^2}$$

$$= 4kT\omega^2 C_d^2 R_s + 2eI_d + \frac{4kT}{|A(\omega)|^2} \left[\frac{\theta(\omega C_o)^2}{g_m} + \frac{1}{R_r} + \frac{\Gamma g_m + \frac{1}{R_L}}{|g_m Z_o|^2} \right],$$

where

$$\frac{1}{Z_o} = \frac{1}{R_r} + j\omega \left(C_o + \frac{C_d}{1 + j\omega C_d R_s} \right),$$

$$C_o = C_{gs} + C_{gd},$$

and R_L is the amplifier load resistance. Thus,

$$S_{\text{eq}} \approx 4kT \left[\omega^2 C_d^2 R_s + \frac{1 + \omega^2 C_d^2 R_s^2}{R_r} + \frac{\theta(\omega C_o)^2}{g_m} (1 + \omega^2 C_d^2 R_s^2) \right.$$

$$+ \frac{\Gamma g_m + \frac{1}{R_L}}{g_m^2} \left\{ \left(\frac{1}{R_r} - \omega^2 C_o C_d R_s \right)^2 \right.$$

$$\left. \left. + \omega^2 \left(C_i + C_d \frac{R_s}{R_r} \right)^2 \right\} \right] + 2eI_d, \quad (14)$$

where

$$C_i = C_d + C_{gs} + C_{gd}.$$

In practice R_r can be made extremely large so

$$\frac{R_s}{R_r} \ll 1$$

and, from eq. (9),

$$\overline{i_{\text{eff}}^2} = 2eI_d f_b g_o + 4kT f_b \left[\left[\frac{1}{R_r} + \frac{\Gamma g_m + \frac{1}{R_L}}{g_m^2 R_r^2} \right] g_o \right.$$

$$+ (2\pi f_b)^2 \left\{ g_o + \frac{\Gamma g_d + \frac{1}{R_L}}{g_m^2} C_i^2 \right\} g_2$$

$$\left. + (2\pi f_b)^4 \left\{ \frac{\Gamma g_d + \frac{1}{R_L}}{g_m^2} C_i^2 + g_o C_d^2 R_s^2 \right\} g_4 \right]. \quad (15)$$

From this relation, it is clear that, from the standpoint of thermal noise, R_r should be as large as possible, even if signal integration takes place.

For junction field-effect transistors such as the 2N3823, the gate noise is negligible. Assuming R_r is large and the detector leakage current is negligible gives the simple relation

$$\overline{i_{\text{eff}}^2} = \frac{8kTf_b(2\pi f_b C_t)^2 g_m}{3g_m} \quad (16)$$

Thus, for this case which is typical for junction FETs operating at a bit rate below 25 Mb/s, the quantity

$$\frac{\sqrt{g_m}}{C_t}$$

is a figure of merit for the required power without avalanche gain. Under the above assumption, the effective noise current increases with the $\frac{3}{2}$ power of the bit rate.

We now turn our attention to the bipolar transistor. Unlike the FET, for a bipolar transistor the optimum bias is dependent on frequency. For a bipolar transistor,

$$S_{\text{eq1}} = 2eI_b, \\ S_{\text{eq2}} = \frac{2eI_c + \frac{4kT}{R_L}}{|g_m Z_b|^2},$$

where Z_b , the impedance across the base, is given by

$$\frac{1}{Z_b} = \frac{1}{R_b} + j\omega \left(C_b + \frac{C_d}{1 + j\omega C_d R_s} \right)$$

and

$$R_b = \frac{kT}{eI_b}.$$

Assuming that the dc current gain equals the ac current gain, the equivalent noise current spectral density is

$$S_{\text{eq}} = S_s + S_d + \frac{S_{\text{eq1}} + S_{\text{eq2}}}{|A(\omega)|^2} \\ = 2eI_b \left(1 + \frac{1}{\beta} \right) + \frac{4kT}{\beta^2 R_L} + 2eI_d + \omega^2 \left[4kT C_d^2 R_s + 2eI_b C_d^2 R_s^2 \right. \\ \left. + \left(\frac{2eI_b}{\beta} + \frac{4kT}{\beta^2 R_L} \right) \left\{ C_t^2 \left(\frac{kT}{eI_b} \right)^2 + C_d^2 R_s^2 + 2C_d^2 R_s \frac{kT}{eI_b} \right\} \right] \\ + \omega^4 \left(\frac{2eI_b}{\beta} + \frac{4kT}{\beta^2 R_L} \right) C_b^2 C_d^2 R_s^2 \left(\frac{kT}{eI_b} \right)^2.$$

Then

$$\begin{aligned} \overline{i_{\text{eff}}^2} = 2f_b e \left[\left\{ \left(1 + \frac{1}{\beta} \right) I_b + \frac{2kT}{e\beta^2 R_L} + I_d \right\} g_o + (2\pi f_b)^2 \left\{ \frac{2kTC_d^2 R_s}{e} \right. \right. \\ \left. \left. + C_d^2 R_s^2 I_b + \left(\frac{I_b}{\beta} + \frac{2kT}{\beta^2 e R_L} \right) \left[C_i^2 \left(\frac{kT}{eI_b} \right)^2 + C_d^2 R_s^2 + 2C_d^2 R_s \left(\frac{kT}{eI_b} \right) \right] \right\} g_2 \right. \\ \left. + (2\pi f_b)^4 \left\{ \left(\frac{I_b}{\beta} + \frac{2kT}{\beta^2 e R_L} \right) C_d^2 C_b^2 R_s^2 \left(\frac{kT}{eI_b} \right)^2 \right\} g_4 \right]. \end{aligned}$$

At values of base bias which will shortly be shown to lead to minimum effective noise at frequencies up to about 1 GHz,

$$\begin{aligned} \frac{R_s}{R_b} &\ll \frac{1}{2}, \\ (2\pi f_b)^2 C_d^2 C_b^2 R_s^2 g_4 &\ll C_i^2 R_b^2 g_2, \end{aligned}$$

and then

$$\begin{aligned} \overline{i_{\text{eff}}^2} = 2f_b e \left[\left\{ \left(1 + \frac{1}{\beta} \right) I_b + \frac{2kT}{e\beta^2 R_L} + I_d \right\} g_o \right. \\ \left. + (2\pi f_b)^2 \left\{ \frac{2kTC_d^2 R_s}{e} + \left(\frac{I_b}{\beta} + \frac{2kT}{\beta^2 e R_L} \right) C_i^2 \left(\frac{kT}{eI_b} \right) \right\} g_2 \right]. \quad (17) \end{aligned}$$

The base capacitance is the sum of the diffusion, depletion, and stray capacitances. The diffusion and depletion capacitances increase with base bias and the stray capacitance is bias independent. We will approximate C_i by

$$C_i \approx C_\alpha + C_\beta I_b.$$

The optimum bias current is then found by differentiating $\overline{i_{\text{eff}}^2}$; however, a third-order equation results. Assuming most of the noise originates from the first stage ($R_L \rightarrow \infty$), the optimum bias current is

$$I_{bo} = \frac{kT}{e} \omega_b C_\alpha \sqrt{\frac{g_2}{(1 + \beta)g_o}} \sqrt{\frac{1}{\omega_b^2 C_\beta^2 \left(\frac{kT}{e} \right)^2 g_2 + 1 + (\beta + 1)g_o}}. \quad (18)$$

The second radical is close to unity under most practical conditions (e.g., up to 1 Gb/s with $\beta = 100$, $C_\beta I_b = 1$ pF) and thus I_{bo} is set by the zero bias capacitance. Substituting I_{bo} into $\overline{i_{\text{eff}}^2}$, again assuming all of the noise originates in the transistor, gives

$$\overline{i_{\text{eff}}^2} = \overline{i_{\text{eff}o}^2} \left\{ 1 + \frac{C_\beta I_{bo}}{C_\alpha} \left(1 + \frac{C_\beta I_{bo}}{2C_\alpha} \right) \right\}, \quad (19)$$

where

$$\overline{i_{\text{eff}o}^2} = \frac{8\pi k T f_b^2 C_\alpha}{\sqrt{\beta}} \sqrt{g_o g_2 \left(1 + \frac{1}{\beta}\right)}. \quad (20)$$

The term $C_\beta I_{bo}$ is the diffusion capacitance at optimum bias.

We can now go back and determine correction terms for the noise contributed by the series and load resistance terms at I_{bo} . The ratio of the effective series noise current to $\overline{i_{\text{eff}o}^2}$ is given by

$$\frac{\overline{i_{\text{eff}s}^2}}{\overline{i_{\text{eff}o}^2}} \approx 2\pi f_b C_d R_s \frac{C_d}{C_\alpha} \sqrt{\frac{g_2}{g_o}} \beta \quad (21)$$

and the ratio of the effective load noise current to $\overline{i_{\text{eff}o}^2}$ by

$$\frac{\overline{i_{\text{eff}L}^2}}{\overline{i_{\text{eff}o}^2}} \approx \frac{4kT}{\beta e R_L I_{bo}}. \quad (22)$$

The input time constant at optimum bias is given approximately by

$$R_b C_t = \frac{C_t}{C_\alpha} \sqrt{\frac{(1 + \beta) g_o}{g_2}} \frac{T_b}{2\pi}. \quad (23)$$

Since $g_o > g_2$ and $\beta \gg 1$ for practical conditions, the time constant will greatly exceed the bit interval. Finally, the current gain at optimum bias is given by

$$G(\omega) = \frac{\beta}{1 + j \frac{\omega C_t}{\omega_b C_\alpha} \sqrt{\frac{(1 + \beta) g_o}{g_2}}}.$$

Thus the transfer function is a function of ω/ω_b and, for a fixed pulse shape and β , the frequency dependence of the current gain, $A(\omega)$, scales with bit rate and its magnitude is independent of bit rate.

V. EXPERIMENTAL RESULTS

The preceding analysis will now be compared with experimental results that have been obtained by Goell at 6.3 Mb/s and 274 Mb/s and by Runge at 50 Mb/s.

The 6.3- and 50-Mb/s repeaters employed 50-percent-duty-cycle rectangular return-to-zero (RZ) optical pulses. For 274 Mb/s, the optical pulses were nonreturn-to-zero (NRZ). For the 6.3-Mb/s repeater the baseband pulses were RZ and for the other two repeaters the baseband signal was NRZ. In all of the cases the baseband pulses were close to the shape to be expected with a raised-cosine spectrum,

Table I — Signal formats and pulse shape integrals

	Transmitted Pulse	Equalized Pulse	\mathcal{J}_0	\mathcal{J}_2
Case I	50 percent duty cycle	RZ	0.30	0.13
Case II	50 percent duty cycle	NRZ	0.40	0.036
Case III	NRZ	NRZ	0.55	0.085

but with some intersymbol interference at the highest bit rate. For the purpose of this paper we shall assume a raised-cosine spectrum. Since the error rate is a rapid function of the signal level, the effect of intersymbol interference on error rate can be accounted for by a reduction of received average power equal to the reduction of the worst-case pulse-pattern signal to threshold level. The integrals \mathcal{J}_0 and \mathcal{J}_2 are summarized for each of the signaling formats in Table I.

For the 6.3-Mb/s and 50-Mb/s repeaters, SiFET front ends were employed. In the former case, g_m was 0.006 mho and the total circuit capacitance 8 pF and for the latter these parameters were 0.006 mho and 6.7 pF, respectively. For the 274-Mb/s repeater two front ends were tested; the first with a common-emitter followed by a common-collector stage, the second with a common-source GaAsFET input stage followed by an emitter follower. In both cases the input capacitance was 4 pF. The bipolar transistor used was an FMT4000.

Figure 5 shows the base current vs collector current for the FMT4000. The current gain for this device is 160 for base currents to well below 1 μ A.

Both the calculated and measured effective noise current is shown in Fig. 6 for the FMT4000. The experimental values were inferred from the power which gave the signal-to-noise ratio experimentally determined to give a 10^{-9} error probability. Experimental curves are given for the input transistor and for the complete receiver. At very low bias currents the noise originating after the first stage becomes significant. Near optimum bias, which was calculated to be 5.5 μ A, the required signal is increased by about 0.5 dB by noise originating after the first stage.

The measured optimum for the first stage is about 4 μ A indicating the base noise is somewhat higher than assumed in the theory. The error-rate performance was found to be optimum at about 7 μ A with about 2½ dB more power than predicted from the calculated first-stage

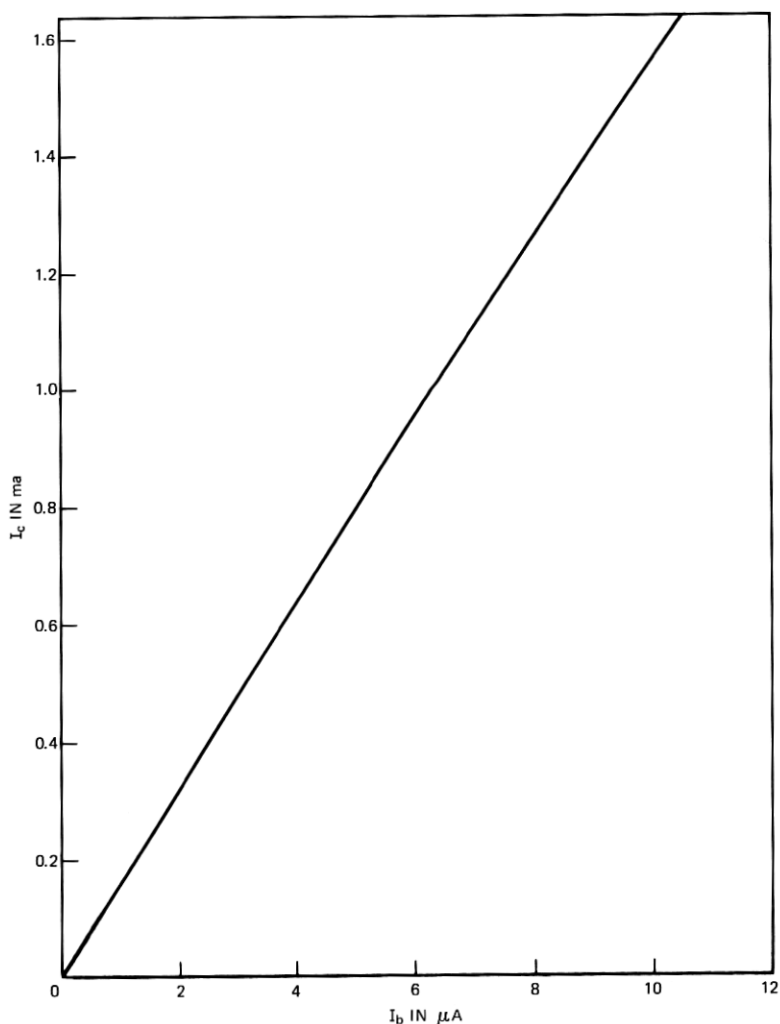


Fig. 5— I_c vs I_b for an FMT4000 bipolar transistor with 10 V collector bias.

and measured subsequent-stage noise. The pulse response for pseudo-random data indicated that about $1\frac{1}{2}$ to 2 dB of this discrepancy were due to intersymbol interference.

The measured and calculated effective noise currents for all of these bit rates are summarized in Table II. For the GaAsFET case an FMT901 transistor was used with a g_m of 0.016 mho. The leakage was

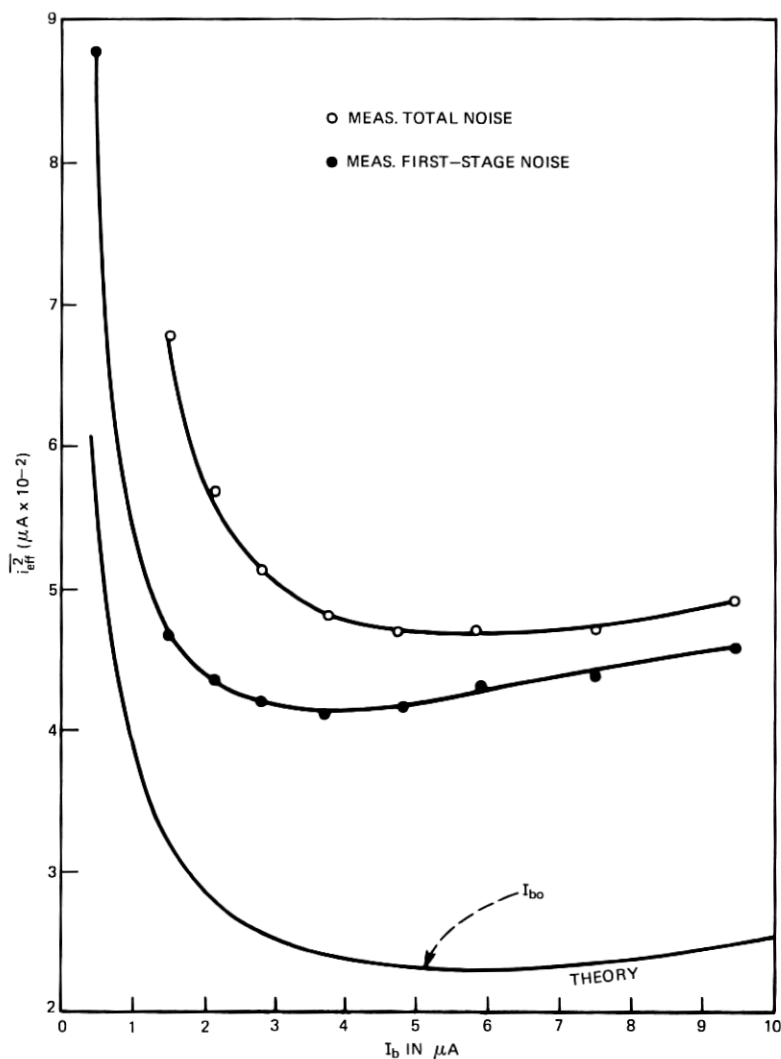


Fig. 6—Effective noise current vs base bias current for an FMT4000 bipolar transistor.

under 1 μA , which is negligible for 274 Mb/s. Only about half the total noise originated in the GaAsFET. This accounts for a significant part of the error. The noise of the later stages could have been reduced by the inclusion of an extra stage in the front end. However, the performance would still have been inferior to that of a bipolar transis-

Table II — Comparative performance

Bit Rate (Mb/s)	Transmitted Pulse Shape	Equalized Pulse Shape	Device	g_m (mmho)	β	C_t	Measured Total $\sqrt{i_{eff}^2}$ (nA)	Measured First Stage $\sqrt{i_{eff}^2}$ (nA)	Calculation $\sqrt{i_{eff}^2}$ (nA)
6.3	50% RZ	RZ	SiFET	6		8.0	0.46	0.40	0.39
50	50% RZ	NRZ	SiFET	6.4		6.7	4.2	*	3.68
274	NRZ	NRZ	BP		160	4	49	42	23
274	NRZ	NRZ	GaAsFET	16		4	79	55	36

* Not available.

tor. The theoretical and experimental effective noise currents shown in Table II for the 6.3-Mb/s and 50-Mb/s cases are in close accord with theory.

VI. COMPARISON OF DEVICES

Several considerations enter into the selection of an input stage for an optical receiver. Among these factors are sensitivity, dynamic range, power consumption, temperature stability, and cost. Each of these factors, with the exception of the last which is beyond the scope of this paper, will now be discussed.

Equations (15) and (20) indicate that the effective noise for bipolar transistors and field-effect transistors without leakage have a different dependence on frequency. Since the rate of noise increase with frequency is lowest for bipolar transistors one would expect them to be best at high frequencies. At lower frequencies FETs could be expected to be superior. GaAsFETs have appreciable leakage currents. With the FMT901 transistor the leakage varies between 0.1 and 100 μ A, though it is typically below 10 μ A. Thus the noise performance degrades at low frequencies. In addition, $1/f$ noise may be a problem. To date little is known about this source of noise in GaAsFETs and the possibility of its being significant at bit rates on the order of 10 Mb/s cannot as yet be ruled out.

Figure 7 illustrates the dependence of the noise of SiFETs, GaAsFETs, and bipolar transistors as a function of frequency. The leakage current noise, shown separately, must be added to the device noise to get the total circuit noise. This is especially important for GaAsFETs where the leakage of the device can be the limiting factor.

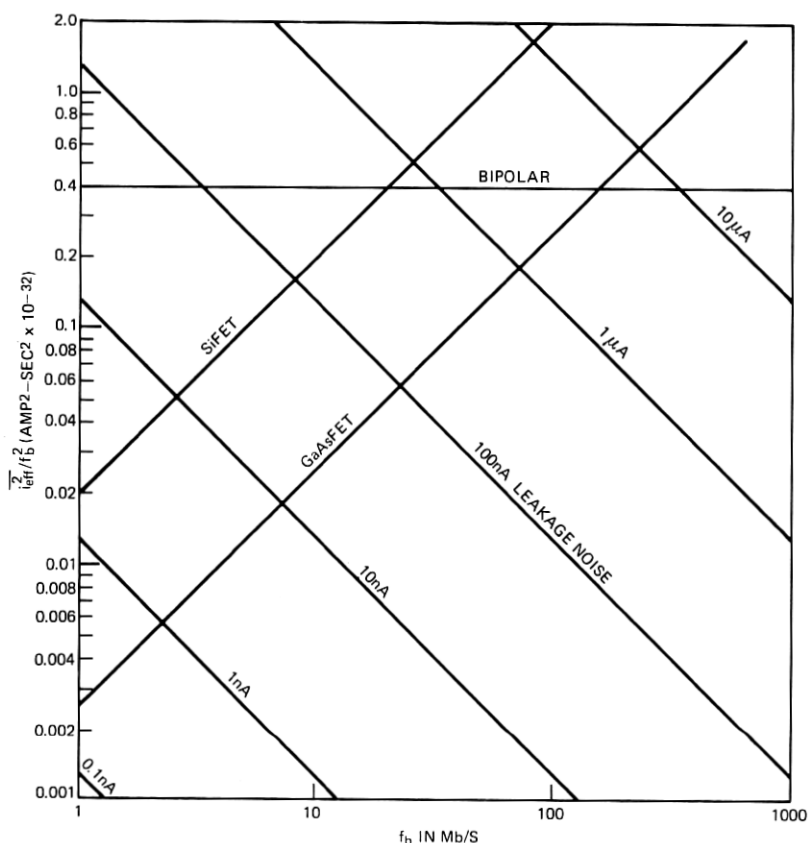


Fig. 7—Effective noise current vs bit rate.

The second case of Table I (50-percent-duty-cycle optical pulses, NRZ baseband) is chosen to illustrate the behavior to be expected. It is assumed that the device parameters of Table III apply. The FET curves terminate at the frequency where $g_m Z_1 = 1$. From the curves for this case bipolar transistors are superior to GaAsFETs above 150 Mb/s and to SiFETs above 20 Mb/s. If leakage were negligible, the GaAsFET would be superior to the SiFET. However, since for currently available devices the leakage runs from about 0.1 to 100 μ A it must be taken into account in the determination of the relative merit of the GaAsFET. For example, with 0.2 μ A of leakage the GaAsFET is superior to the SiFET above about 5 Mb/s. Unless the leakage is below about 1 μ A it is never superior to the bipolar transistor.

Table III — Device parameters for Fig. 7

Device	C_t (pF)	g_m (mho)	β
Bipolar Transistors	4		160
SiFET	8	0.005	
GaAsFET	4	0.016	

The previous cases apply to readily achievable results with commercial devices. However, these devices are not optimized for optical receiver applications. Figure 8 shows the optimum bias as a function of bit rate for each of the cases of Table I. The optimum bias current is extremely small and for many transistors the beta will start to drop before optimum is reached. By reducing the area of devices the range

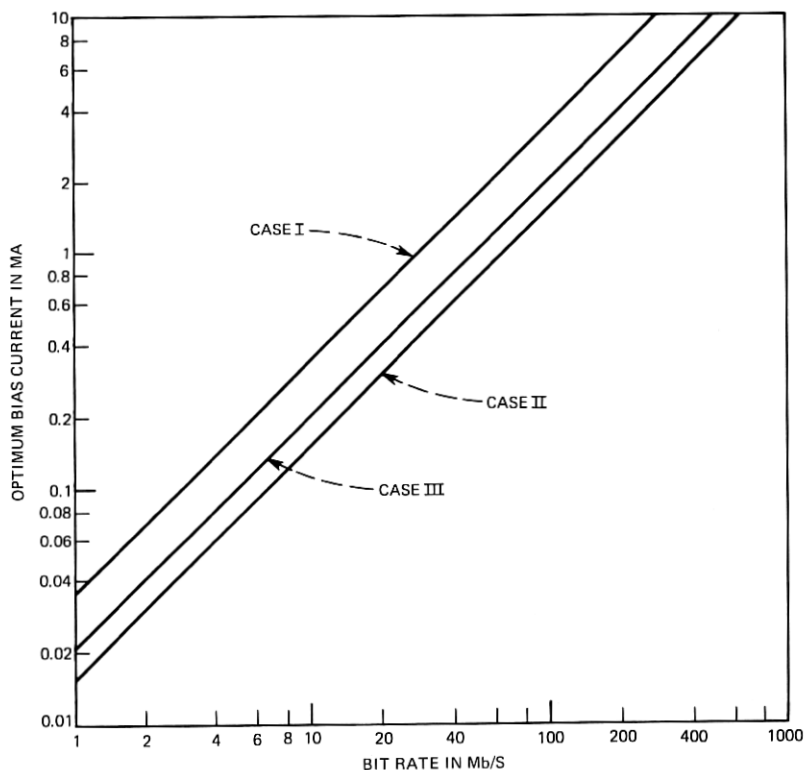


Fig. 8—Optimum bias vs bit rate.

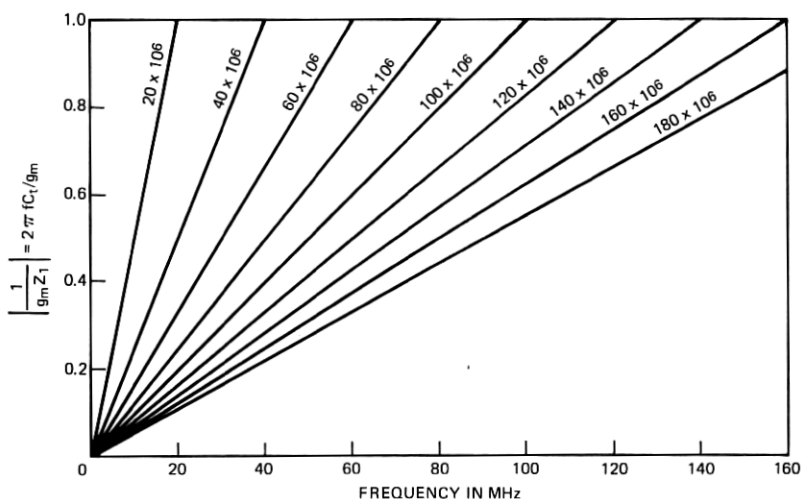


Fig. 9—Reciprocal gain vs frequency with gain bandwidth product ($g_m/2\pi C_t$) as a parameter.

of operation can be extended. Furthermore, it will reduce the capacitance. If the stray and detector capacitances can also be reduced an additional improvement in performance can be achieved.

The upper frequency at which an FET can be used is set by the gain bandwidth product of the device in the circuit. Figure 9 shows the gain versus frequency with $g_m/2\pi C_t$ as a parameter. With an integrating second stage the second-stage noise becomes insignificant if the reciprocal gain, $1/g_m Z_1$, at the highest frequency of interest is below 0.5 while for the noise from a nonintegrating second stage to be insignificant the reciprocal gain must be below about 0.1 at the highest frequency of interest.

For an FET, g_m and C_g are both proportional to gate length.* Increasing gate length increases drain noise ($g_m/C_g^2 \propto 1/\text{length}$). On the other hand, decreasing gate length reduces the total capacitance more slowly than g_m due to the detector and stray capacitance and thus increases the noise contribution of the succeeding stages. Thus an optimum value exists† which can be determined from eq. (15) or eq. (14) if the load noise is frequency independent.

* Gate length refers to the dimension perpendicular to current flow and width to the direction of current flow. The former dimension is readily changed. The latter can press the technology.

† G. L. Miller has recently pointed out that $C_g = C_d$ is the optimum condition when the first-stage drain noise predominates.

With improving technology it is expected that the gate width can be significantly reduced. Typical commercial silicon devices with 5- μm gate widths have gain bandwidth products of 132 MHz; experimental devices with 0.5- μm gate widths have been reported with a gain bandwidth product near 1 GHz.¹⁰

We will now direct our attention to the question of dynamic range. Without avalanche gain, for an ac-coupled FET the voltage swing at the detector for the required minimum signal increases with the square root of the reciprocal bit rate. This effect has not been fully analyzed and data are not presently available indicating the bit rate at which amplitude distortion prevents proper equalization. However, at 6.3 Mb/s, problems were not encountered with the signal 10 dB above that required for 10^{-9} error rate.

For a bipolar transistor the signal current can become comparable with the bias current leading to gain variations with word pattern for an integrating front end. For example, with a -31-dBm signal (10^{-9} error rate at 274 Mb/s) without avalanche gain the signal current is about 0.4 μA average. Since the optimum bias is near 5 μA this is appreciable. The ratio $\sqrt{i_{\text{eff}}^2}/I_{bo}$ is proportional to $1/\sqrt{C_\alpha}$ and independent of frequency. Thus the ratio of the required minimum signal current to bias current is frequency independent, but can be expected to increase as C_α decreases.

If C_α could be greatly reduced so that

$$\sqrt{i_{\text{eff}}^2} \gg I_{bo}$$

then the bias could be turned off and integration would not take place. The noise would only be present when the signal was on and would be given by

$$S_{\text{eq}}^2 = 2eI_{\text{signal}}.$$

This expression is identical to the one which applies to ideal photo-multipliers and avalanche detectors with an infinite electron/hole ionization coefficient and large gain; the required signal is 3 dB above the quantum limit.

Present bipolar transistors have a higher transconductance-to-device-current ratio than an FET. Thus, they consume less power. With avalanche gain where the required optical power is relatively insensitive to amplifier noise (varies at $\frac{1}{2}$ root), supply power may often be the deciding factor. It has recently been suggested that FETs have the same limiting transconductance-to-current ratio as bipolar

transistors,¹¹ e/kT . However, as yet this limit is not approached under practical considerations.

Finally, bipolar transistors operated well above the reverse saturation current have better temperature stability than FETs. In applications employing dc coupling this could be an important consideration.

APPENDIX

The equivalent input noise current spectral density of a cascade of circuits is calculated as follows. First, the circuits are partitioned in any convenient manner. Next, the output impedance of each stage is found going from the input to the output of the cascade since the output impedance is a function of the input loading. Next, the contribution of the equivalent noise current of each stage is referred to the input by dividing it by the product of the short-circuit current gains of all of the preceding stages. Finally, the individual contributions are summed in the square sense, that is,

$$S_{eq} = S_{eq}^1 + \sum_{i=2}^n S_{eq}^i \prod_{j=1}^{i-1} \frac{1}{|A_j^2(\omega)|}, \quad (24)$$

where $A_j(\omega)$ is the short-circuit current gain of the j th stage and S_{eq}^i is the value of S_{eq} for the i th stage.

The current gain, output impedance, and contribution to S_{eq} of S_1 and S_2 (S_{eq1} and S_{eq2}) for the common emitter (source), base (gate), and collector (drain) configurations are summarized in Table IV in terms of the common emitter (source) parameters. The primed and subscripted impedances are the parallel combination of the impedance

Table IV — Equivalent parameters

Configuration (Common Terminal)	Equivalent Noise Due to S_1 - S_{eq1}	Equivalent Noise Due to S_2 - S_{eq2}	Current gain $A(\omega)$	Output Impedance
Emitter (source)	S_1	$\frac{S_2}{g_m Z_1' \left(\frac{Z_2 - 1}{g_m} \right) / (Z_1' + Z_2)}$	$-g_m Z_1' \left(\frac{Z_2 - 1}{g_m} \right) / (Z_1' + Z_2)$	$Z_1' \left[\frac{Z_1' + Z_2}{Z_1' + Z_2 + Z_1 + g_m Z_1' Z_2} \right]$
Base (gate)	S_1	$\frac{Z_2 S_2}{Z_1' + g_m Z_1' Z_2}$	$\frac{Z_1' + g_m Z_1' Z_2}{Z_1' + Z_2 + g_m Z_1' Z_2}$	$Z_2 \frac{Z_1' + Z_2 + g_m Z_1' Z_2}{Z_1' + Z_2 + Z_1 + g_m Z_1' Z_2}$
Collector (drain)	$\frac{Z_1(g_m Z_2' - 1)S_1}{Z_2'(g_m Z_1 + 1)}$	$\frac{(Z_1 + Z_2)S_2}{Z_2'(1 + g_m Z_1)}$	$\frac{Z_2(1 + g_m Z_1)}{Z_1 + Z_2'}$	$Z_3 \frac{Z_1 + Z_2'}{Z_1 + Z_2' + Z_3 + g_m Z_1 Z_3}$

with the same subscript and the output impedance of the preceding stage.

When

$$Z_2 > Z'_1, Z_3, Z'_1 + Z_3$$

and

$$Z_2 \gg 1/g_m$$

the common emitter (source) and base (gate) configurations give appreciable current gain. Under this condition the approximate relations of Table V apply for S_{eq1} , S_{eq2} , A , and Z_o emitter (source) and base (gate) stages; and for S_{eq1} , S_{eq2} , and A for a common collector (drain) stage. Table V also gives approximate parameters for output impedance for a common collector (drain) stage for the cases

$$g_m Z_1 \gg 1, \quad Z'_2 \gg Z_1$$

and

$$Z'_2 \ll g_m Z_1 Z_3, \quad Z'_2 \ll Z_1.$$

The first case is typical of bipolar and the second of field-effect transistors. The \parallel symbol represents the parallel combination of impedances.

Insight into the choice of circuit configuration can be gained by examining the results given in Table V when the preceding assumptions apply. If the gain of a single stage is large enough that the noise of subsequent stages is negligible, then all three configurations give identical results for S_{eq1} and S_{eq2} . For this case, the choice of configuration would be made on the basis of output impedance. Since the detector impedance, except at extremely high frequencies, is large, a common base (gate) stage can usually be ruled out and the selection

Table V — Approximate equivalent parameters

Configuration (Common terminal)	S_{eq1}	S_{eq2}	$A(\omega)$	Z_o
Emitter (Source)	S_1	$\frac{S_2}{g_m(Z_s \parallel Z_1)}$	$-g_m(Z_s \parallel Z_1)$	Z_3
Base (Gate)	S_1	$\frac{S_2}{g_m(Z_s \parallel Z_1)}$	1	$g_m Z'_1 Z_3$
Collector (Drain)	S_1	$\frac{S_2}{g_m(Z_s \parallel Z_1)}$	$g_m(Z_s \parallel Z_1)$	$Z_3 \parallel \frac{Z'_2}{g_m Z_1}$ (Case I) $\frac{1}{g_m}$ (Case II)

between the common emitter (source) and common collector (drain) stage made on the basis of desired output impedance. Parenthetically, it is interesting to note that the output voltage for the two cases is identical—the first gives voltage gain but the second presents a higher impedance to the source.

For multistage amplifiers a cascode configuration [common emitter (source) stage followed by a common base (gate) stage] is often chosen for the first two stages. A cascode amplifier has a wider bandwidth than a common emitter (source) stage and thus can simplify equalization. However, it does not lead to the lowest total noise since $A \approx 1$ for a common base (gate) stage and therefore the full value of S_{eq1} for the following stage contributes to the equivalent noise spectral density.

The approach which gives the lowest equivalent noise is a cascade of common emitter (source) stages—possibly followed by a common collector (drain) stage to match impedance—because common emitter (source) stages exhibit the current gain of common collector (drain) stages, but present a higher output impedance to the following stage, thereby minimizing the second-stage S_{eq2} contribution to S_{eq} .

REFERENCES

1. H. Melchior and W. T. Lynch, "Signal and Noise Response of High Speed Germanium Avalanche Photodiodes," IEEE Trans. Elec. Dev., *ED-13*, No. 12 (December 1966), pp. 829-838.
2. S. D. Personick, "Receiver Design for Digital Fiber Optic Communication Systems, I," B.S.T.J., *52*, No. 6 (July-August 1973), pp. 843-875.
3. A. B. Gillespie, *Signals, Noise, and Resolution in Nuclear Counter Amplifiers*, New York: McGraw-Hill, 1953.
4. O. H. Schade, Sr., "A Solid-State Low-Noise Preamplifier and Picture-Tube Drive Amplifier for a 60 MHz Video System," RCA Review, *29*, No. 1 (March 1968), p. 3.
5. J. E. Goell, "An Optical Repeater With High-Impedance Input Amplifier," B.S.T.J., *53*, No. 4 (April 1974), pp. 629-643.
6. P. Runge, private communication.
7. A. van der Ziel, *Noise: Sources, Characterization, Measurement*, Englewood Cliffs, N. J.: Prentice-Hall, 1970.
8. Das B. MuKunda, "FET Noise Sources and Their Effects on Amplifier Performance at Low Frequencies," IEEE Trans. Elec. Dev., *ED-19*, No. 3 (March 1972), pp. 338-348.
9. W. Baechtold, "Noise Behavior of GaAs Field-Effect Transistor with Short Gate Lengths," IEEE Trans. Elec. Dev., *ED-19*, No. 5 (May 1972), pp. 674-680.
10. W. Baechtold, K. Dactwyler, T. Forster, T. O. Mohr, W. Walter, and P. Wolf, "Si and GaAs 0.5 μ m-Gate Schottky-Barrier Field Effect Transistors," Elec. Letters, *9*, No. 10 (May 17, 1973), pp. 232-234.
11. F. O. Johnson, "The Insulated Gate Field-Effect Transistor—A Bipolar Transistor in Disguise," RCA Review, *34*, No. 3 (March 1973), pp. 80-94.

